Hindawi Publishing Corporation
Journal of Nanomaterials
Volume 2011, Article ID 573429, 7 pages
doi:10.1155/2011/573429

Research Article

Synthesis of Plant-Mediated Silver Nanoparticles Using *Dioscorea batatas* Rhizome Extract and Evaluation of Their Antimicrobial Activities

P. C. Nagajyothi and K. D. Lee

Department of Nanomaterial Chemistry, Dongguk University, Gyeongju 780-714, Republic of Korea

Correspondence should be addressed to K. D. Lee, kdlee@dongguk.ac.kr

Received 20 April 2011; Revised 24 May 2011; Accepted 8 June 2011

Academic Editor: Ugur Serincan

The eco-friendly synthesis of nanoparticles through various biological means helps to explore various plants for their ability to synthesize silver nanoparticles (AgNPs). Here we have synthesized AgNPs by using rhizome extract of *Dioscorea batatas* at 80°C as well as room temperature (25°C). AgNPs were characterized under UV-vis spectrophotometer, SEM, FTIR, XRD, and EDX. The antimicrobial activity of AgNPs was evaluated on gram positive (*B. substilis* and *S. aureus*), gram negative (*E. coli*), and fungi (*S. cerivisae* and *C. albicans*). At room temperature, *S. cerivisae* and *C. albicans* were found to be more susceptible to AgNPs than at 80°C.

1. Introduction

Biosynthesis provides advancement over chemical and physical method as it is cost effective, environment friendly, and easily scaled up for large-scale synthesis and obviates the need for high pressure, energy, temperature, and toxic chemicals [1, 2]. Large-scale production by chemical and physical methods usually results in particles larger than several micrometers while the biological synthesis can be successfully used for production of small nanoparticles in large-scale operations [3].

The use of silver and other metal ions for their sustained antifungal, antibacterial and antiviral effects has been practiced from antiquity. Recent studies have focused on the synthesis of homogenous AgNPs and evaluation of their antimicrobial activities [4, 5]. Silver ion has been known to be effective against a broad range of microorganisms. Antimicrobial activities of AgNPs have been reported by various researchers [6, 7]. Ingle and coworkers [8] found that AgNPs exhibited significant antimicrobial activity against *Escherichia coli* and multidrug resistant *Staphylococcus aureus*, and Pal et al. [9] reported that the antibacterial activity of AgNPs against the gram-negative *E. coli* depends on the shape of the nanoparticles. Kim et al. [10, 11] reported that spherical AgNPs showed potent activity against *Trichophyton mentagrophytes, Trichosporon beigelii*, and *Candida albicans* compared with that of commercially available antifungal agents (amphotericin B and fluconazole).

Dioscorea grows extensively on mountains as well as in fields within Korea and Japan. In the present study AgNPs were synthesized using *Dioscorea* rhizome (Figure 1) and characterized with various characterization techniques. The antimicrobial activity of AgNPs was investigated against various pathogenic gram positive and gram negative bacterial and fungal species.

2. Material and Methods

2.1. Synthesis of AgNPs Using Dioscorea Rhizome Extract. *Dioscorea* rhizomes were collected from Gyeongju-oriental medical college, Gyeongju, South Korea. The rhizomes were air dried for 10 days and then kept in a hot air oven at 60°C for 24 hours. Rhizomes were ground to fine powder. 1 mM silver nitrate ($AgNO_3$) purchased from Sigma-Aldrich Chemical Pvt. Ltd. was added to rhizome extract to make up a final solution 200 mL. A change in the color of solution was observed during the heating process.

Figure 1: *Dioscorea batatas* rhizome.

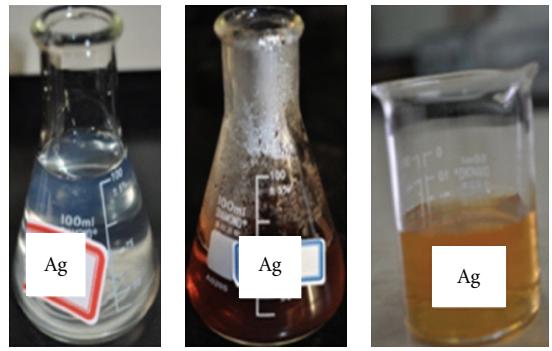

(a) (b) (c)

Figure 2: Color change of rhizome extracts containing AgNPs before and after synthesis: (a) before synthesis, (b) at 80°C, and (c) at 25°C.

2.2. UV-Vis Spectrophotometer Analysis. The reduction of pure Ag^+ ions was monitored by measuring the UV-vis spectrum of the reaction medium at 5 hours after diluting a small aliquot of the sample into distilled water. UV-vis spectral analysis was done by using UV-vis spectrophotometer (Cary 4000 UV-vis spectro photometer).

2.3. SEM and EDX Analysis. The biomass after reaction spontaneously precipitated at the bottom of the conical flasks in 1 hours. After the precipitation, the suspension above the precipitate was sampled for SEM-EDX observations. SEM samples of the aqueous suspension of nanoparticles were fabricated by dropping the suspension onto clean electric glass and allowing water to completely evaporate. Samples were coated by carbon and SEM analyses were performed on a Hitachi s-3500N.

2.4. XRD Analysis. The AgNPs solutions were purified by repeated centrifugation at 5000 rpm for 20 minutes followed by redispersion of the pellet of AgNPs into 10 mL of deionized water. After freeze drying of the purified nanoparticles, the structure and composition were analyzed by XRD (Rigaku RINT 2100 series). The dried mixture of AgNPs was collected for the determinutesation of the formation of AgNPs by an X'Pert Pro X-ray diffractometer operated at a voltage of 40 kV and a current of 30 mA with Cu Kα radiation in a θ-2θ configuration.

2.5. FTIR Analysis. To remove any free biomass residue or compound that is not the capping ligand of the nanoparticles, the residual solution of 100 mL after reaction was centrifuged at 5000 rpm for 10 minutes and the resulting suspension was redispersed in 10 mL sterile distilled water. The centrifuging and redispersing process was repeated three times. Thereafter, the purified suspension was freeze dried to obtain dried powder. Finally, the dried nanoparticles were analyzed by FTIR (Bruker model, TENSOR 37).

2.6. Antimicrobial Assays. Synthesized AgNPs were tested for antimicrobial activity by agar disc-diffusion method

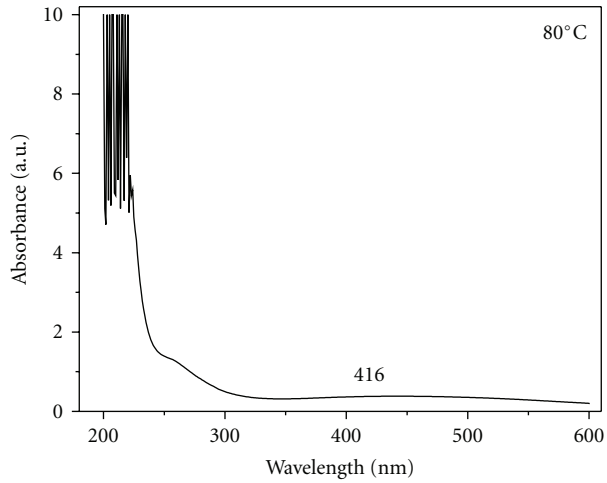

(a)

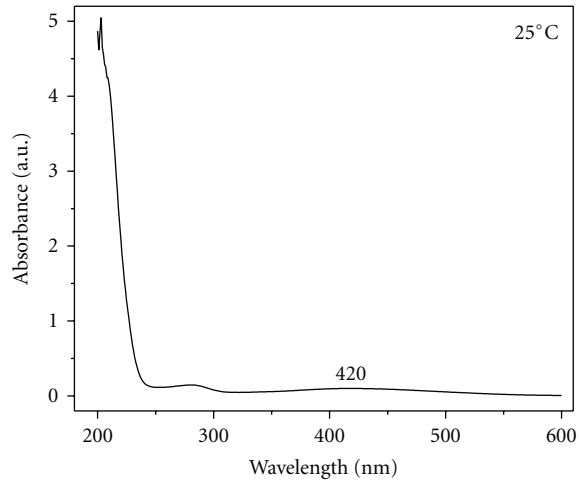

(b)

Figure 3: UV-vis absorption spectrum of AgNPs (a) at 80°C and (b) at 25°C.

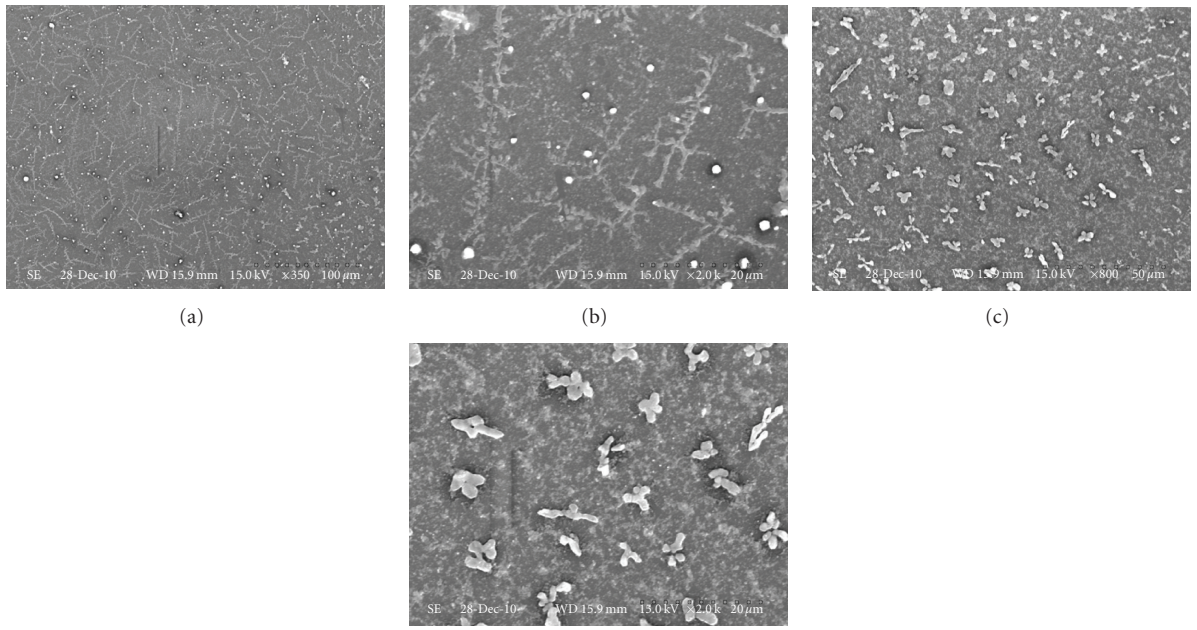

Figure 4: SEM images of the biosynthesized of AgNPs showing at different magnifications: (a) and (b) AgNPs at 80°C; (c) and (d) AgNPs at 25°C.

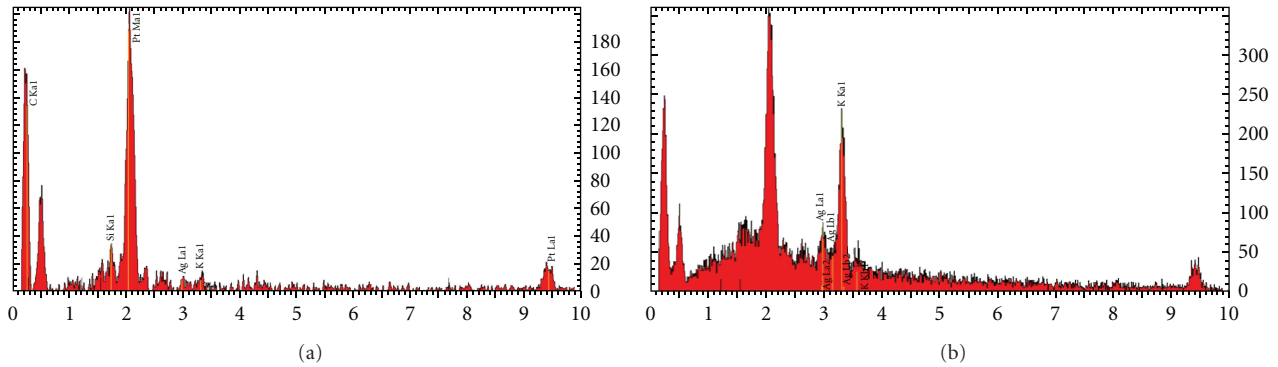

Figure 5: EDX spectrum of AgNPs (a) at 80°C and (b) at 25°C.

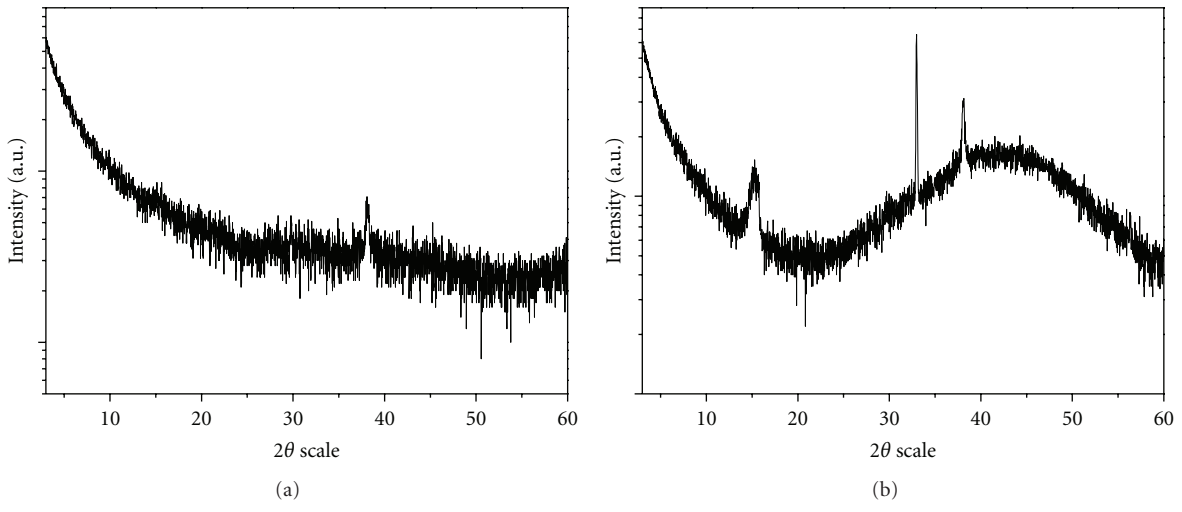

Figure 6: XRD spectrum of AgNPs (a) at 80°C and (b) at 25°C.

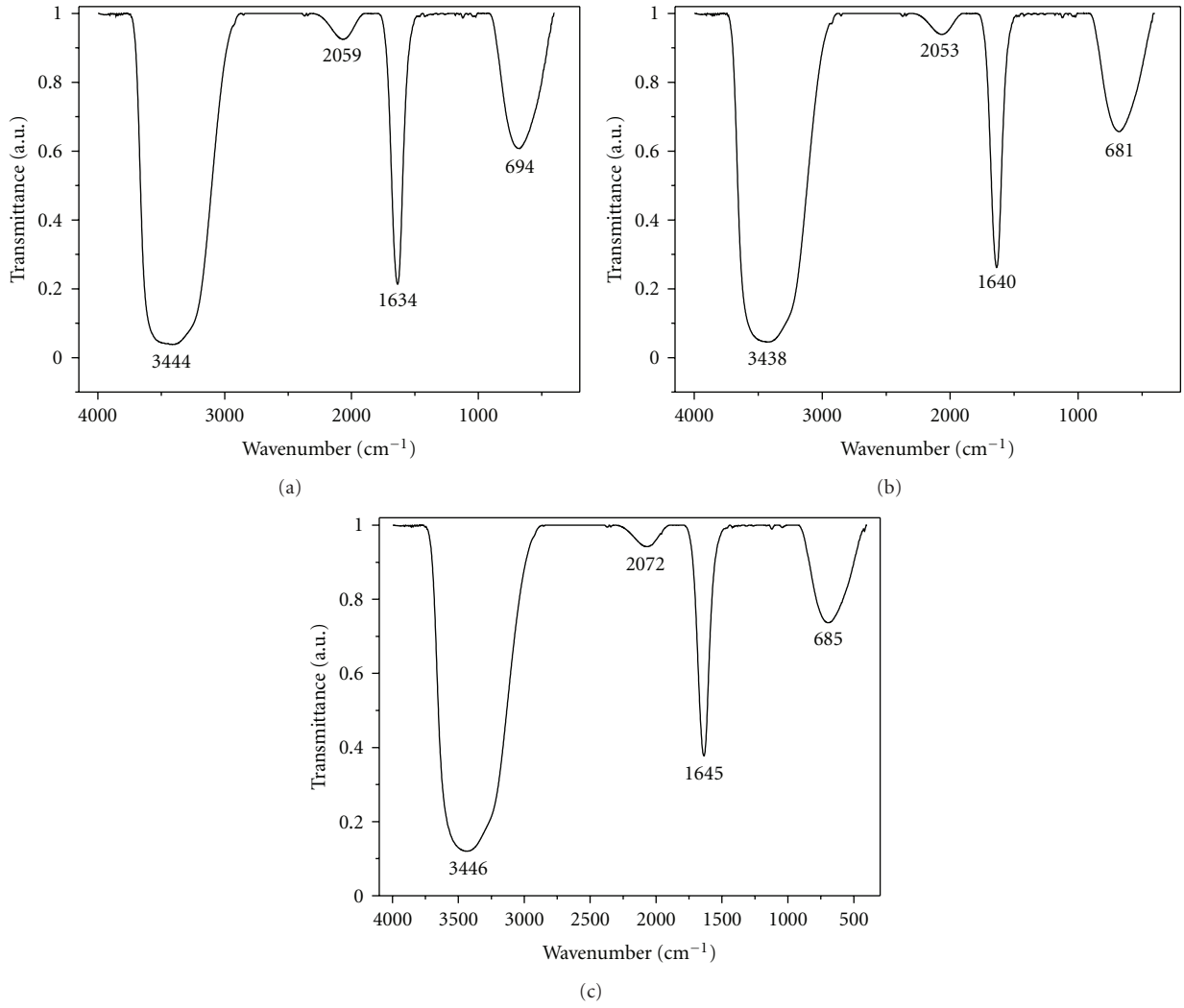

Figure 7: FTIR spectrum of AgNPs: (a) *Dioscorea batatas* rhizome extract, (b) at 80°C, and (c) at 25°C.

against pathogenic bacteria, *B. subtilis*, *S. aureus* and *E. coli*, and pathogenic fungi *C. albicans* and *S. cerevisiae*. Pure cultures of bacterial and fungal pathogens were subcultured on Mueller Hinton and Potato Dextrose Agar (PDA), respectively. The microbial test organisms were grown in nutrient broth at 37°C for 24 hours. A 500 μL aliquot of each organism (1×10^6 cfu/mL) was spread on agar using a cotton swab and allowed to dry for 10 minutes. Paper discs loaded with 50 μg/mL AgNPs and reference drugs were placed on the surface of each cultured plate and incubated at 37°C for 24 hours after which inhibition zones were measured [12]. Experiments were conducted in duplicate and mean results recorded.

3. Results and Discussion

3.1. UV-Vis Spectro Photometer Study. Bioreduction of aqueous Ag^+ ions can easily be followed by UV-vis spectro photometer, and one of the most important features in optical absorbance spectra of metal nanoparticles is surface plasmon band, which is due to collective electron oscillation around the surface mode of the particles. Previous studies have shown that silver exhibits yellowish-brown color due to the excitations of their surface plasmon response (SPR) [13], when dissolved in water. The color of the solution changes from colorless to brownish yellow, within 50 minutes at 80°C and dark yellow; this reaction takes up to 2 hours for completion at room temperature (Figures 2(a)–2(c)). The possible explanation of difference in the reduction time could be due to the difference in their reduction potential for both the metal ions.

Metal nanoparticles such as silver and gold have free electrons, which gives rise to SPR absorption band [14]. The characteristic SPR resonance band of biogenic AgNPs occurred at 420 nm and 416 nm for reaction carried out at 80°C and room temperature, respectively, (Figures 3(a)-3(b)). The reactants are consumed rapidly eventually leading to the formation of smaller nanoparticles [15, 16].

3.2. SEM and EDX Studies. Figures 4(a)–4(d) show the SEM images of the synthesized AgNPs. The overall morphology of

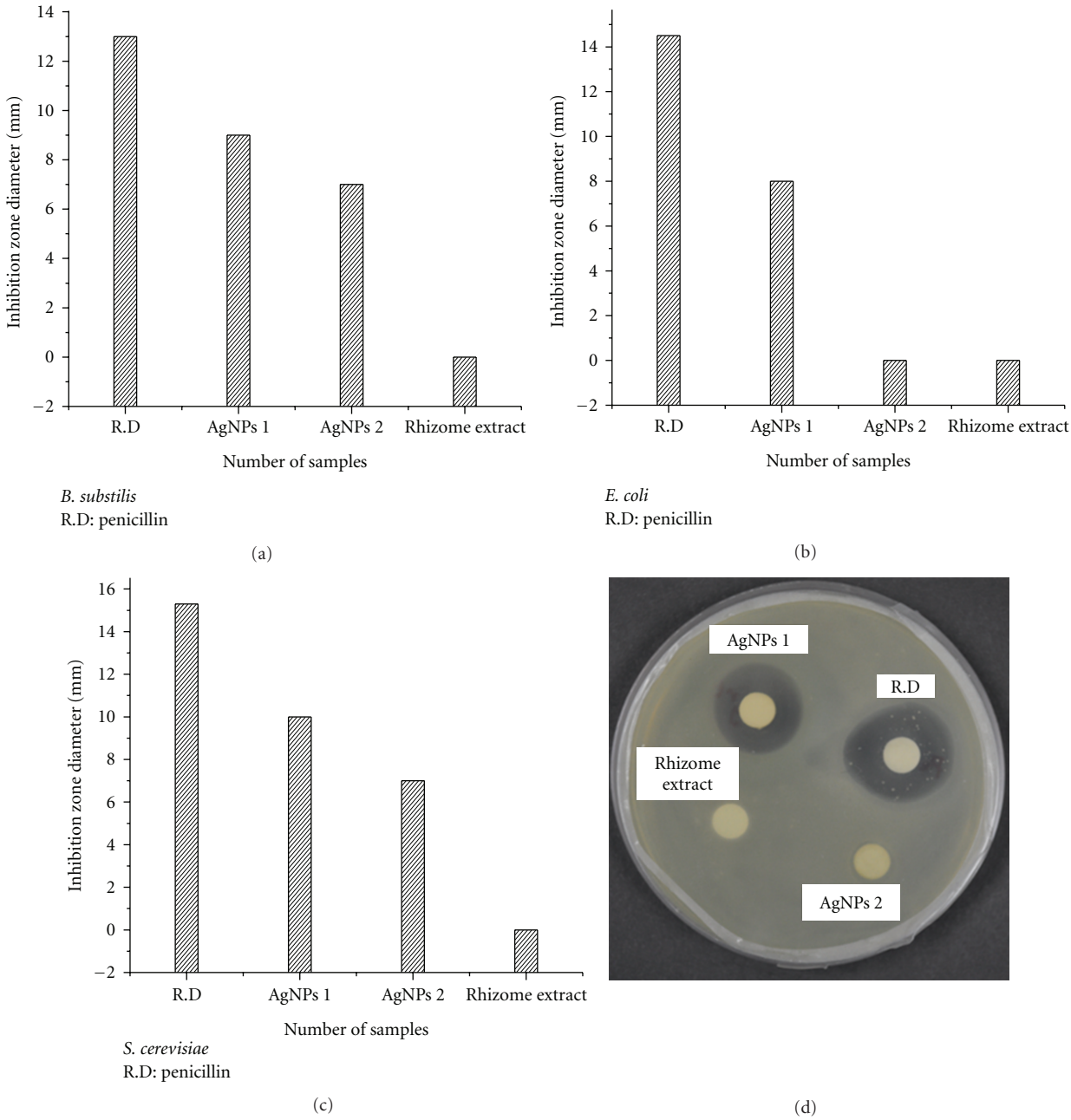

Figure 8: (a)–(d) Zones of inhibition of the growth of *B. substilis* (lab culture), *E. coli* (KCTC 2441), and *S. cerevisiae* (lab culture) and upon application of reference drug (penicillin). Diagrams show the averaged inhibition-zone diameters for samples. R.D: reference drug; AgNPs 1: at room temperature; AgNPs 2: at 80°C.

AgNPs is more clearly seen, and the particles are monodispersed, having circular and flower shapes, respectively, at 80°C and 25°C.

Figures 5(a)-5(b) show the EDX spectrum of AgNPs synthesized at 25°C and 80°C. Strong signals from the silver atoms in the nanoparticles were observed, and signals from Si, K, C, and Pt atoms were also recorded. The C and K signals were likely due to X-ray emission from carbohydrates/proteins/enzymes present in the cell wall of the biomass. Metallic AgNPs generally show typical absorption peak approximately at 3 KeV due to SPR [17]. The presence of the elemental silver can be observed in the graph obtained from EDX analysis, which also supports the XRD results.

3.3. XRD and FTIR Studies. The XRD pattern of the AgNPs is shown in Figures 6(a) and 6(b). Various Bragg reflections clearly indicated the presence of (111) and (200) sets of lattice planes and further on the basis that they can be indexed as face-centered-cubic (FCC) structure of silver. Hence from the XRD pattern it is clear that AgNPs formed using *Dioscorea* rhizome broth were essentially crystalline

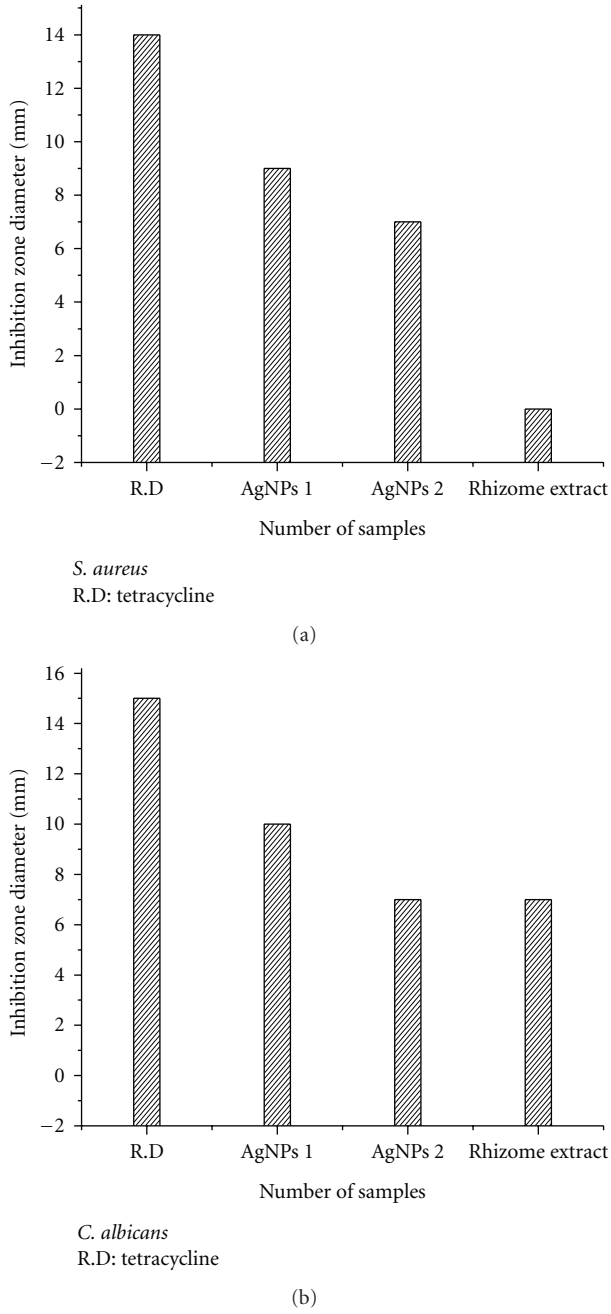

Figure 9: (a) and (b) Zones of inhibition of the growth of *S. aureus* (KCTC 1916) and *C. albicans* (lab culture), and upon application of reference drug (tetracycline).

in nature. In addition to the Bragg peaks representative of FCC AgNPs, additional as yet unassigned peaks are also observed suggesting that the crystallization of bio-organic phase occurs on the surface of the nanoparticles.

FTIR results reveal absorption bands at 3444, 1634, and 694 cm^{-1} (rhizome extraction) in Figure 7(a); 3438, 1640, and 681 cm^{-1} (AgNPs at 80°C) in Figure 7(b); 3446, 1645, and 685 cm^{-1} (AgNPs at 25°C) in Figure 7(c), respectively. The vibrational bands correspond to the bonds such as aminuteso (N–H), –C=C (alkene), and C–Cl (Halogens) which were in the region range of 673–3446 cm^{-1}. The most wide spectrum absorption was observed at 3444 and 13446 cm^{-1} and it can be attributed to the stretching vibrations of aminuteso (N–H) [18]; absorption peaks centered at 1640 and 1645 cm^{-1} can be attributed to the stretching vibration of –C=C (alkene) [19].

3.4. Antimicrobial Activity of AgNPs. Antimicrobial effect of AgNPs was examinutesed on gram positive *S. aureus* and *B. substilis*, gram negative *E. coli*, and fungal strains: *C. albicans* and *S. cerevisae*. The results consigned in Figures 8(a)–8(d) and 9(a)-9(b) are indicative of the diameters of zones of inhibition due to microbial susceptibility. AgNPs exerted highest toxicity against *C. albicans* and *S. cerevisae* intermediary effects on *S. aureus* and *B. substilis* and exhibited the lowest effect on *E. coli*. The order of susceptibility to the metal nanoparticles can be written as fungi > gram positive > gram negative. The AgNPs at 25°C showed more inhibitory activity on microbes compared to AgNPs at 80°C. AgNPs were found to be significantly toxic against the fungal and gram positive microbes and exhibited mild toxicity against *E. coli*. AgNPs were more effective against gram positive bacterial strains than the gram negative bacteria strains [18]. Ag^+ ions uncouple the respiratory chain from oxidative phosphorylation or collapse the proton-motive force across the dependent on the size and shape of NPs [10]. Morones et al. [20] reported that AgNPs were preferentially bound to the cytoplasmic membrane. In addition to that, the pitting of the AgNPs caused in the bacterial cell wall is also responsible for the death of bacteria. The actual bacteria mechanism of AgNPs is not well known, some researchers agree that silver releases Ag^+ ions, and they interact with thiol groups of bacterial proteins affecting the replication of DNA [21].

4. Conclusion

Rapid and green synthesis shows that the environmentally benign and renewable rhizome of *Dioscorea batatas* can be used as an effective capping as well as reducing agent for the synthesis of AgNPs. The spectroscopic characterizations from UV-vis spectro photometer, FTIR, and SEM support the formation and stability of the biosynthesized AgNPs. Further, the above AgNPs revealed to possess an effective antimicrobial property against *C. albicans* and *S. cerevisae*. The present study emphasizes the use of plants medicinal for the synthesis of AgNPs with potent antimicrobial effect. Synthesis of metallic nanoparticles using green resources like *Dioscorea batatas* rhizome is a challenging alternative to chemical synthesis, since this novel green synthesis is a pollutant free and eco-friendly synthetic route for the synthesis.

References

[1] V. Bansal, D. Rautaray, A. Ahmad, and M. Sastry, "Biosynthesis of zirconia nanoparticles using the fungus *Fusarium oxysporum*," *Journal of Materials Chemistry*, vol. 14, no. 22, pp. 3303–3305, 2004.

[2] S. Senapati, A. Ahmad, M. I. Khan, M. Sastry, and R. Kumar, "Extracellular biosynthesis of bimetallic Au-Ag alloy nanoparticles," *Small*, vol. 1, no. 5, pp. 517–520, 2005.

[3] T. Klaus, R. Joerger, E. Olsson, and C. G. Granqvist, "Silver-based crystalline nanoparticles, microbially fabricated," *Proceedings of the National Academy of Sciences of the United States of America*, vol. 96, no. 24, pp. 13611–13614, 1999.

[4] P. Mehrbod, N. Motamed, M. Tabatabaian et al., "In vitro antiviral effect of "nanosilver" on influenza virus," *Daru*, vol. 17, no. 2, pp. 88–93, 2009.

[5] A. R. Shahverdi, A. Fakhimi, H. R. Shahverdi, and S. Minaian, "Synthesis and effect of silver nanoparticles on the antibacterial activity of different antibiotics against *Staphylococcus aureus* and *Escherichia coli*," *Nanomedicine*, vol. 3, no. 2, pp. 168–171, 2007.

[6] A. R. Shahverdi, A. Fakhimi, H. R. Shahverdi, and S. Minaian, "Synthesis and effect of silver nanoparticles on the antibacterial activity of different antibiotics against *S. aureus* and *Escherichia coli*," *Nanomedicine*, vol. 3, no. 2, pp. 168–171, 2007.

[7] J. S. Kim, E. Kuk, K. N. Yu et al., "Antimicrobial effects of silver nanoparticles," *Nanomedicine*, vol. 3, no. 1, pp. 95–101, 2007.

[8] A. Ingle, A. Gade, S. Pierrat, C. Sönnichsen, and M. Rai, "Mycosynthesis of silver nanoparticles using the fungus *Fusarium acuminatum* and its activity against some human pathogenic bacteria," *Current Nanoscience*, vol. 4, no. 2, pp. 141–144, 2008.

[9] S. Pal, Y. K. Tak, and J. M. Song, "Does the antibacterial activity of silver nanoparticles depend on the shape of the nanoparticle? A study of the gram-negative bacterium *Escherichia coli*," *Applied and Environmental Microbiology*, vol. 73, no. 6, pp. 1712–1720, 2007.

[10] K. J. Kim, W. S. Sung, S. K. Moon, J. S. Choi, J. G. Kim, and D. G. Lee, "Antifungal effect of silver nanoparticles on dermatophytes," *Journal of Microbiology and Biotechnology*, vol. 18, no. 8, pp. 1482–1484, 2008.

[11] K. J. Kim, W. S. Sung, B. K. Suh et al., "Antifungal activity and mode of action of silver nano-particles on *Candida albicans*," *BioMetals*, vol. 22, no. 2, pp. 235–242, 2009.

[12] C. Perez, M. Pauli, and P. Bazerque, "An antibiotic assay by the agarwelldiffusion method," *Acta Biologiae et Medecine Experimentalis*, vol. 15, pp. 113–115, 1990.

[13] P. Mulvaney, "Surface plasmon spectroscopy of nanosized metal particles," *Langmuir*, vol. 12, no. 3, pp. 788–800, 1996.

[14] M. A. Noginov, G. Zhu, M. Bahoura et al., "The effect of gain and absorption on surface plasmons in metal nanoparticles," *Applied Physics B*, vol. 86, no. 3, pp. 455–460, 2007.

[15] J. Y. Song and B. S. Kim, "Rapid biological synthesis of silver nanoparticles using plant leaf extracts," *Bioprocess and Biosystems Engineering*, vol. 32, no. 1, pp. 79–84, 2009.

[16] D. Raghunandan, S. Basavaraja, B. Mahesh, S. Balaji, S. Y. Manjunath, and A. Venkataraman, "Biosynthesis of stable polyshaped gold nanoparticles from microwave-exposed aqueous extracellular anti-malignant guava (*psidium guajava*) leaf extract," *Nanobiotechnology*, vol. 5, no. 1–4, pp. 34–41, 2009.

[17] P. Magudapathy, P. Gangopadhyay, B. K. Panigrahi, K. G. M. Nair, and S. Dhara, "Electrical transport studies of Ag nanoclusters embedded in glass matrix," *Physica B*, vol. 299, no. 1-2, pp. 142–146, 2001.

[18] I. Maliszewska and Z. Sadowski, "Synthesis and antibacterial activity of of silver nanoparticles," *Journal of Physics: Conference Series*, vol. 146, Article ID 012024, 2009.

[19] P. Rajasekharreddy, P. U. Rani, and B. Sreedhar, "Qualitative assessment of silver and gold nanoparticle synthesis in various plants: a photobiological approach," *Journal of Nanoparticle Research*, vol. 12, no. 5, pp. 1711–1721, 2010.

[20] J. R. Morones, J. L. Elechiguerra, A. Camacho et al., "The bactericidal effect of silver nanoparticles," *Nanotechnology*, vol. 16, no. 10, pp. 2346–2353, 2005.

[21] M. Marini, S. De Niederhausern, R. Iseppi et al., "Antibacterial activity of plastics coated with silver-doped organic-inorganic hybrid coatings prepared by sol-gel processes," *Biomacromolecules*, vol. 8, no. 4, pp. 1246–1254, 2007.